In-situ crystal structure determination of seifertite SiO_2 at 129 GPa: studying a minor phase near Earth's core–mantle boundary

Li Zhang[1,*], Dmitry Popov[2], Yue Meng[2], Junyue Wang[1,3], Cheng Ji[1,4], Bing Li[1,4], Ho-kwang Mao[1,3]

[1]Center for High Pressure Science and Technology Advanced Research (HPSTAR), Shanghai 201203, China;
[2]High Pressure Collaborative Access Team (HPCAT), Geophysical Laboratory, Carnegie Institution of Washington, Argonne, IL 60439;
[3]Geophysical Laboratory, Carnegie Institution of Washington, Washington, DC 20015;
[4]High Pressure Synergetic Consortium (HPSynC), Geophysical Laboratory, Carnegie Institution of Washington, Argonne, IL 60439;

*zhangli@hpstar.ac.cn

Seifertite SiO_2 likely exists as a minor phase near the core–mantle boundary. Simulating the pressure and temperature conditions near the core–mantle boundary, seifertite was synthesized as a minor phase in a coarse-grained, polycrystalline sample coexisting with the $(Mg,Fe)SiO_3$ post-perovskite phase at 129 GPa and 2500 K. Here we report the first *in-situ* single-crystal structure determination and refinement of seifertite at high pressure and after a temperature quench from laser heating. We improved the data coverage of a minor phase from a diamond anvil cell by merging single-crystal data of seifertite from six selected grains which had different orientations. Observed systematic absences of reflections from the six individual grains allowed only one space group: *Pbcn*. The refined results of seifertite are in good agreement with the predictions from previous first-principles calculations at high pressure. This approach provides a method of structure determination of a minor phase in a mineral assemblage synthesized under *P*-*T* conditions representative of the deep Earth.

Key words: high pressure; crystal structure; multigrain; SiO_2; seifertite; synchrotron X-ray; deep mantle

Earth's core–mantle boundary (CMB) is located at approximately 2900 km beneath the surface, corresponding to pressures (*P*) of 136 GPa and temperatures (*T*) greater than 2500 K. The major lower-mantle phase, iron-bearing magnesium silicate $(Mg,Fe)SiO_3$ perovskite, transforms to a different, compact orthorhombic post-perovskite (pPv) phase at *P-T* conditions near the CMB (Murakami et al., 2004; Oganov and Ono, 2004), providing a possible explanation for the distinct seismic features in the D″ layer above the CMB. SiO_2 is a common mineral in the Earth's crust, and silicates comprise most of the mantle. Free SiO_2 may also exist in the mantle through subduction of mid-ocean ridge basalt (MORB) crust (Andrault et al., 2014; Hirose et al., 2005). Under pressure (*P*) and temperature (*T*) conditions relevant to the Earth's lower mantle, SiO_2 transforms from stishovite to $CaCl_2$-type at ~50 GPa and room temperature (Cohen, 1992; Kingma et al., 1994), then to α-PbO_2 like structure known as seifertite (EL Goresy et al., 2008) at *P-T* conditions near the CMB (Dubrovinsky et al., 1997; Grocholski et al., 2013). Knowing the accurate crystal structure of seifertite at relevant *P–T* conditions is fundamentally important for understanding the deep mantle.

The space group of seifertite has been under debate due to the similarity of the systematic absences of several space groups (Belonoshko et al., 1996; Dera et al., 2002; Dubrovinsky et al., 1997; Karki et al., 1997a; Karki et al., 1997b; Teter et al., 1998; Tse et al., 1992; Tsuchida and Yagi, 1990). When the phase was first experimentally discovered in a DAC (Dubrovinsky et al., 1997), the few peaks observed in the powder XRD pattern did not allow unambiguous structure determination, and thus the study assumed the theoretical predication of space group *Pnc2 (Belonoshko et al., 1996)*. A post-stishovite phase of SiO_2 was also discovered in the Shergotty Meteorite (Sharp et al., 1999), and the powder X-ray diffraction

(XRD) data of this meteorite sample suggested the space group *Pbcn.* (Dera et al., 2002). However, the study also pointed out that the power XRD pattern alone could not unambiguously conclude the centrosymmetric structure (Dera et al., 2002). Later first principles calculations came to agreement on the space group *Pbcn* (Karki et al., 1997a; Karki et al., 1997b; Teter et al., 1998). Recent powder diffraction data provide further constraints on the phase boundary between the $CaCl_2$ and α-PbO_2 like phases of SiO_2 and their equations of state up to 152 GPa and 3500 K in a laser-heated DAC using noble gas media (Grocholski et al., 2013). To date, however, an unambiguous structure determination of seifertite within its stability field has not yet been achieved, due to the challenges in structure studies at ultrahigh pressure. Seifertite appears as a minor phase in the run product at *P-T* conditions representative of the CMB when MORB or Fe-rich orthopyroxene are used as the starting material, and such sample environments may influence the crystal chemistry of seifertite (Hirose et al., 2005). In this study, seifertite was also synthesized as a minor phase in a coarse-grained polycrystalline mineral assemblage coexisting with $(Mg,Fe)SiO_3$ pPv. We then applied the multigrain approach (Sørensen et al., 2012) to obtain the first single-crystal structure determination and unambiguous refinement of seifertite under conditions representative of the CMB.

Structure determination of a minor phase in a multiphase assemblage

Powder X-ray diffraction (XRD) in a DAC has intrinsic limitations when the sample consists of multiple phases with low symmetries. For instance, the natural MORB sample decomposed to four phases at *P-T* condition representative of the CMB: $MgSiO_3$-rich pPv, α-PbO_2-type SiO_2, Ca-perovskite and $CaFe_2O_4$-type Al-phase (Hirose et al., 2005). Overlapping peaks in such a powder XRD pattern make

phase indexation and structure determination challenging in high-pressure mineralogical studies. On the other hand, single-crystal XRD provides a more definitive characterization of a crystal structure at high pressure. To achieve good reciprocal space coverage from a single-crystal in a DAC, efforts have been made to maximize the DAC opening while still maintaining high pressure. For instance, an X-ray aperture of 85° was achieved at pressure up to 50 GPa for this purpose (Boehler, 2006). Still, maintaining such a wide X-ray access angle becomes challenging at higher pressure. Even in a successful single-crystal DAC experiment, only a portion of the reciprocal space can be illuminated by X-rays (Miletich et al., 2000). Meanwhile, a single pre-selected crystal (or several) can only be maintained in a soft pressure-transmitting medium of He or Ne to a certain pressure. At elevated pressures, preloaded single crystals either become degraded or break into polycrystallites when passing through a phase transition. In high-pressure petrological studies, multiple phases coexist in a polycrystalline sample as a result of phase equilibrium, and the structure determination and crystal chemistry of each phase is fundamentally important for understanding the phase relations in such system. However, new structures and minor phases are often overshadowed by the diffraction of major phases in a powder diffraction pattern, and are impossible to identify. Therefore, the structure determination of a minor phase in such a multiphase assemblage has never previously been possible using conventional single-crystal or powder diffraction techniques.

Utilization of the multigrain method (Sørensen et al., 2012) for a polycrystalline sample in a DAC has opened a new area for high-pressure crystallography at megabar pressures (Nisr et al., 2012; Zhang et al., 2013). The multigrain approach also allows the separation of crystallographic information of an unknown phase from a mixture at

high pressure (Zhang et al., 2014). As the X-ray beams available at synchrotron facilities tend to be very focused and intense, most of the powder XRD patterns will show some degree of spottiness. Heating a powder sample can further promote spottiness in a powder XRD pattern due to crystal growth at high temperature. Spottiness, which is generally considered as a flaw in a powder XRD, can be turned into great advantage if we can handle the diffraction patterns from many individual crystallites as if they were from isolated single crystals. While successful demonstration for crystal structure refinement in a polycrystalline sample at ambient conditions using the multigrain approach (Schmidt et al., 2003; Vaughan et al., 2004), an ideal single-crystal can often be obtained at ambient conditions for the use of conventional single-crystal techniques. On the other hand, the multigrain approach shows great advantages for *in-situ* studying a polycrystalline sample at high pressure by determining an individual orientation matrix for each individual grain, allowing high-pressure crystallographic studies unachievable using conventional single crystal techniques. In this study, we demonstrate a solution for structure determination of a minor phase within a multiple phase assemblage at high pressures representative of the CMB.

Synthesis of seifertite as minor phase and its unit cell parameters

In this study, an orthopyroxene sample with $(Mg_{0.6}Fe_{0.4})SiO_3$ composition and ~5% excess of SiO_2 was used as the starting material. The starting material was pre-compressed into disks of ~10 μm thickness and cut to ~40 μm in diameter and placed in a rhenium (Re) gasket hole in a Mao-type symmetric DAC filled with Ne. Diamond anvils with flat culet diameters of 120 μm beveled at 10° up to 300 μm were mounted in Boehler seats with up to 60° X-ray opening. The micro-focused x-ray diffraction with *in-situ* laser heating available at 16IDB at the Advanced Photon Source (APS) of

Argonne was used to study changes in the sample at *P*-*T* conditions representative of the CMB. Temperatures were measured on both sides by spectroradiometry (Shen et al., 2001) and pressures were determined from the unit-cell volumes of Ne (Fei et al., 2007) after *T* quench from laser heating.

Free silica crystallized in seiferite as a minor phase above 118 GPa and 2500 K, but remained as $CaCl_2$-type structure at 111 GPa and 2500 K, suggesting a narrow depth for the existence of seifertite in the lowermost mantle. This result is consistent with the most recent study in which SiO_2 was mixed with a metal absorber (Grocholski et al., 2013). The coarse-grained polycrystallites of seifertite were obtained in a quasihydrostatic environment of Ne after laser heating, and showed highly spotty XRD patterns within the 5–8μm focused X-ray microbeam.

Seifertite was again synthesized at 129 GPa and 2500 K in a DAC that offers a opening angle of $4\theta > 50°$. The unit-cell parameter of Ne after *T* quench was 2.903(8) Å calculated from four diffraction lines 111, 200, 220 and 311. Figure 2(A) and 2(B) show seifertite as a minor phase coexisting with pPv and the characteristic peak 110 at 2.90 Å and 111 at 2.39 Å were identified for seifertite. Over 40,000 diffraction spots were obtained from the XRD patterns collected by rotating the DAC from -24° to 24° at steps of 0.2°. Such a small angular step was used in order to improve the signal-to-noise ratio by reducing the background level. The exposure time was 20 sec/frame. The FABLE package (Sørensen et al., 2012) was used to filter the spots, and GrainSpotter (Schmidt, 2014) in the package was used to assign the reflections to each of the specific orientation matrices. Over one hundred grains were identified, but most are too fine for structure analysis. Only those with maximum number of reflections were selected for further structure studies.

Multigrain patterns show great advantages for separating reflections with close *d*-spacings and picking up weak reflections when compared to powder XRD patterns with smooth rings. Figure 3 shows three pairs of diffraction reflections from one selected grain of seifertite. In a 2D powder XRD pattern, the {302} diffraction ring with *d*-spacing of 1.067 Å would overlap with {321} with 1.061 Å; in a multigrain pattern, however, each of the reflections can be unambiguously identified through its unique rotation, Bragg and azimuth angles, as shown in Figure 3(A) and 3(B). Additionally, weak diffraction peaks are often overshadowed by the background noise in a smooth powder XRD pattern; in contrast, a couple of diffraction spots contribute to most of the intensity of a diffraction peak in a multigrain pattern, and, therefore, weak reflections, such as the {421} reflections shown in Figure 3(C), can be picked out, despite having only a few pixels slightly more intense than the background.

In the powder pattern most peaks at high *d*-spacing were overshadowed by the strong peaks from the major phase pPv (Figure 2(B)), only one characteristic peak of seifertite (2.90 Å) was observed in the low *d*-spacing region. On the other hand, the multigrain approach allows us to calculate the unit-cell parameters from multiple grains through three-dimensional orientation and geometrical relationships. Table 1 shows the calculated unit-cell parameters from four individual grains and merged grains using the software UNITCELL (Holland and Redfern, 1997). The unit cell parameters of seifertite at 129 GPa are: a=3.7277(2) Å, b=4.6576(2) Å, c=4.1609(3) Å, V=72.243(5) Å. The standard deviations for the calculated unit-cell parameters are found to be nearly inversely proportional to the square root of the number of reflections, demonstrating our measurements statistically robust. The uncertainties in *d*-values are mainly defined by resolution of the monochromator. The unit-cell volume obtained in this study is 1.1% higher than the volume from previous powder

XRD data at 129 GPa (Grocholski et al., 2013), corresponding to a pressue difference of ~6 GPa, likely due to the difference between the Au and Ne pressure scales. The *a/b* and *a/c* ratios are in reasonable agreement with our results because the ratios are not pressure sensitive due to the compact configuration of the seiferite structure. The *a/b* and *a/c* ratios from another powder XRD study (Murakami, 2003) are 3.7 and 1.0% lower than the values obtained from our study, respectively, probably due to the non-hydrostatic environment in the previous study. In comparison with powder diffraction, the multigrain approach provides a solution for accurate calculations of unit-cell parameters, especially for a minor phase in a mineral assemblage where multiple phases coexist.

Structure determination and refinement of seifertite

Intensities of reflections from each selected grain have been calculated using the XDS software (Kabsch, 2010). This program uses very efficient integration and scaling algorithms, but it assumes that reflections from only one crystal are present on X-ray images. That was why, among all the diffraction spots identified by XDS, only those from a selected crystalline grain had to be selected. For this purpose a pair of reflections from this grain was previously identified using the FABLE package. Indices and coordinates of these two reflections were used to calculate the orientation matrix (Busing and Levy, 1967) which in turn allowed us to identify all the reflections belonging to this grain. Some specifically developed software was implemented for this purpose. All further data processing by XDS was done as normal, assuming there was only one crystal in the beam. XDS does not allow the definition of shaded areas changing during the data collection routine. That was why reflections shaded by the DAC were recognized by XDS as having intensities below the detectable level. Such reflections have been removed, by another program we developed, from the output

listings after the integration, based on the orientation and opening of the DAC. Calibration of sample-to-detector distance and detector tilt was done based on a diffraction pattern from CeO_2 powder standard using Fit2d software (Hammersley et al., 1996). CrysAlis (Oxford Diffraction Ltd, 2006) and other softwares may also be used for integration and scaling purpose and considered for future.

As the available number of reflections from a single-crystal was limited by its DAC opening, data from six individual grains with the maximum number of available reflections have been used to determine the space group of seifertite at 129 GPa. Observed systematically absent reflections allowed only space group: *Pbcn* (#60), confirming the prediction by theory (Karki et al., 1997a; Karki et al., 1997b; Teter et al., 1998). The same six grains were selected for structure solution and refinement. Pole figures shown in Figure 1 represent the random crystallographic orientations of six selected grains. Compatibility between these six data sets has been checked by merging them using the XSCALE software available within the XDS package. In total 613 reflections have been combined providing a redundancy of 6.6. Ten misfits due to overlap of reflections from different grains, overlap with diamond peaks, or locations close to shaded areas have been rejected by XDS automatically. Data completeness of 92.1% was achieved in the *d*-spacing range down to 0.72Å, approaching nearly full access to a reflection sphere of the structure. The position of Si was determined from a Patterson map, and coordinates of O were obtained from a difference in electron density map calculated after refinement of the Si atomic position. The refinement of the structure was performed against the resulting intensity data of 81 independent reflections using anisotropic thermal parameters. Ten independent reflections were not included into the refinement, but used to calculate R_{free} value which was not affected by overfitting. A reasonable R_{free}=6.4% was obtained. Four misfits have been

rejected from the refinement process. Some more misfits still may be present in the data set; however, their influence on the R-factor is probably reduced due to averaging with the majority of the reflections. All the calculations were performed using the SHELX package (Sheldrick, 2008). Atomic coordinates refined against all these data sets are given in Table 2, while crystallographic data, parameters of the structure refinements, and interatomic distances are given in Table 3 and are compared to the structure data from previous theoretical calculations at high pressure (Karki et al., 1997a; Karki et al., 1997b; Teter et al., 1998) and to the powder XRD data of the meteorite sample at ambient conditions (Dera et al., 2002). The refined structure results at 129 GPa are in good agreement with previous theoretical calculations at 120 GPa (Karki et al., 1997a; Karki et al., 1997b; Teter et al., 1998). However, when structures become more complicated, theory and experiment may show different strengths: as theoretical calculations can reach any pressure range, while experimental approaches may better handle complicated chemistry.

Implications

The space group *Pbcn* (#60) of seifertite was unambiguously determined based solely on the observed systematically absences of reflections from six differently orientated grains, solving the long-standing controversy. Compared with the structure of seifertite at ambient conditions in a powder meteorite sample (Dera et al., 2002), we found that compression of seifertite is nearly isotropic over the megabar pressure range with a/c=0.91 and b/c=1.12, a property distinct from that of low-pressure polymorphs of SiO_2, such as quartz (Angel et al., 1997) and stishovite (Andrault et al., 2003; Grocholski et al., 2013). The compact configuration of seifertite, especially the short distance between the neighboring unoccupied octahedral voids (Dera et al., 2002), may contribute to such behavior.

Additionally, the unit-cell parameters of seifertite can be precisely determined from hundreds of reflections in a multigrain sample, despite being a minor phase in a mineral assemblage above megabar pressure. Therefore, SiO_2 may serve as a pressure scale in an Fe-bearing sample environment, because other commonly used pressure scales, such as MgO and Pt, often react with Fe-bearing components, especially in high-temperature experiments with heating. However, Al_2O_3 can be incorporated into the seifertite (Grocholski et al., 2013; Hirose et al., 2005), suggesting SiO_2 would not be an ideal pressure scale in Al-bearing compositions.

In this study, the FABLE and XDS packages were bridged in order to determine the structure of a minor phase in a polycrystalline mineral assemblage contained in a DAC. This study demonstrates that the multigrain approach (Sørensen et al., 2012) can be applied to tough data collections for studying phase transitions, crystal chemistry, and chemical reactions in a petrological multiphase system under *P-T* conditions representative of the deep Earth.

ACKNOWLEDGMENTS

We thank J. Smith and S. Sinogeikin for their technical support and G. Shen, S. Schmidt, S. Merkel and A. Katrusiak for their helpful discussions. L. Zhang acknowledges HPSTAR and the Foundation of President of China Academy of Engineering Physics (Grant No: 201402032). The experiment was performed at HPCAT (Sector 16), Advanced Photon Source (APS), Argonne National Laboratory. HPCAT operations are supported by the U.S. Department of Energy–National Nuclear Security Administration (DOE-NNSA) under award DE-NA0001974 and DOE–Basic Energy Sciences (BES) under award DE-FG02-99ER45775, with partial

283 instrumentation funding by NSF. Use of the APS facility was supported by DOE-BES
284 under contract DE-AC02-06CH11357.
285

REFERENCES CITED:

Andrault, D., Angel, R.J., Mosenfelder, J.L., and Le Bihan, T. (2003) Equation of state of stishovite to lower mantle pressures. American Mineralogist, 88, 301-307.

Andrault, D., Pesce, G., Bouhifd, M.A., Bolfan-Casanova, N., Henot, J.M., and Mezouar, M. (2014) Melting of subducted basalt at the core-mantle boundary. Science, 344(6186), 892-5.

Angel, R.J., Allan, D.R., Miletich, R., and Finger, L.W. (1997) The Use of Quartz as an Internal Pressure Standard in High-Pressure Crystallography. Journal of Applied Crystallography, 30, 461-466.

Belonoshko, A.B., Dubrovinsky, L.S., and Dubrovinsky, N.A. (1996) A new high-pressure silica phase obtained by molecular dynamics. American Mineralogist, 81, 785-788.

Boehler, R. (2006) New diamond cell for single-crystal x-ray diffraction. Review of Scientific Instruments, 77(11), 115103.

Busing, W.R., and Levy, H.A. (1967) Angle Calculations for 3- and 4- Circle X-ray and Neutron Diffractometers. Acta Crystallographica, 22, 457-464.

Cohen, R.E. (1992) First-Principles Predictions of Elasticity and Phase Transitions in High Pressure SiO2 and Geophysical Implications. In Y. Syono, and M.H. Manghnani, Eds. High-Pressure Research: Application to Earth and Planetary Sciences. American Geophysical Union, Washington, D. C.

Dera, P., Prewitt, C.T., Boctor, N.Z., and Hemley, R.J. (2002) Characterization of a high-pressure phase of silica from the Martian meteorite Shergotty. American Mineralogist, 87, 1018-1023.

Dubrovinsky, L.S., Saxena, S.K., Lazor, P., Ahuja, R., Eriksson, O., Wills, J.M., and Johansson, B. (1997) Experimental and theorectial indentification of a new high pressure phase of silica. Nature, 388, 362-365.

EL Goresy, A., Dera, P., Sharp, T.G., Prewitt, C.T., Chen, M., Dubrovinsky, L., Wopenka, B., Boctor, N.Z., and Hemley, R.J. (2008) Seifertite, a dense orthorhombic polymorph of silica from the Martian meteorites Shergotty and Zagami. European Journal of Mineralogy, 20, 523-528.

Fei, Y., Ricolleau, A., Frank, M., Mibe, K., Shen, G., and Prakapenka, V. (2007) Toward an internally consistent pressure scale. Proc Natl Acad Sci U S A, 104(22), 9182-6.

Grocholski, B., Shim, S.H., and Prakapenka, V.B. (2013) Stability, metastability, and elastic properties of a dense silica polymorph, seifertite. Journal of Geophysical Research: Solid Earth, 118(9), 4745-4757.

Hammersley, A.P., Svensson, S.O., Hanfland, M., Fitch, A.N., and Hausermann, D. (1996) Two-dimensional detector software: from real detector to idealised image or two-theta scan. High Pressure Research, 14(4-6), 235-248.

Hirose, K., Takafuji, N., Sata, N., and Ohishi, Y. (2005) Phase transition and density of subducted MORB crust in the lower mantle. Earth and Planetary Science Letters, 237(1-2), 239-251.

Holland, T.J.B., and Redfern, S.A.T. (1997) UNIT CELL refinement from powder diffraction data: the use of regression diagnostics. Mineralogical Magazine, 61, 65-77.

Kabsch, W. (2010) Xds. Acta Crystallogr D Biol Crystallogr, 66(Pt 2), 125-32.
Karki, B.B., Warren, M.C., Stixrude, L., Ackland, G.J., and Crain, J. (1997a) Ab initio studies of high-pressure structural transformations in silica. Physical Review B, 55(6), 3465-3471.
-. (1997b) Erratum: Ab initio studies of high-pressure structural transformations in silica. Physical Review B, 56(5), 2884.
Kingma, K.J., Cohen, R.E., Hemley, R.J., and Mao, H.-K. (1994) Transformation of stishovite to a denser phase at lower-mantle pressures. Nature, 374, 243-245.
Miletich, R., Allan, D.R., and Kuhs, W.F. (2000) High-Pressure Single-Crystal Techniques. Reviews in Mineralogy and Geochemistry, 41(1), 445-519.
Murakami, M. (2003) Stability of CaCl2-type and α-PbO2-type SiO2at high pressure and temperature determined by in-situ X-ray measurements. Geophysical Research Letters, 30(5).
Murakami, M., Hirose, K., Kawamura, K., Sata, N., and Ohishi, Y. (2004) Post-perovskite phase transition in MgSiO3. Science, 304(5672), 855-8.
Nisr, C., Ribárik, G., Ungár, T., Vaughan, G.B.M., Cordier, P., and Merkel, S. (2012) High resolution three-dimensional X-ray diffraction study of dislocations in grains of MgGeO3post-perovskite at 90 GPa. Journal of Geophysical Research: Solid Earth, 117(B3), B03201.
Oganov, A.R., and Ono, S. (2004) Theoretical and experimental evidence for a post-perovskite phase of MgSiO3 in Earth's D" layer. Nature, 430, 445-448.
Oxford Diffraction Ltd. (2006) CrysAlis Red.
Schmidt, S. (2014) GrainSpotter: a fast and robust polycrystalline indexing algorithm. Journal of Applied Crystallography, 47(1), 276-284.
Schmidt, S., Poulsena, H.F., and Vaughanb, G.B.M. (2003) Structural refinements of the individual grains within polycrystals and powders. Journal of Applied Crystallography, 36, 326-332.
Sharp, T.G., El Goresy, A., Wopenka, B., and Chen, M. (1999) A Post-Stishovite SiO2 Polymorph in the Meteorite Shergotty: Implications for Impact Events. Science, 284, 1511-1513.
Sheldrick, G.M. (2008) A short history of SHELX. Acta Crystallogr A, 64(Pt 1), 112-22.
Shen, G., Rivers, M.L., Wang, Y., and Sutton, S.R. (2001) Laser heated diamond cell system at the Advanced Photon Source for in situ x-ray measurements at high pressure and temperature. Review of Scientific Instruments, 72(2), 1273-1282.
Sørensen, H.O., Schmidt, S., Wright, J.P., Vaughan, G.B.M., Techert, S., Garman, E.F., Oddershede, J., Davaasambuu, J., Paithankar, K.S., Gundlach, C., and Poulsen, H.F. (2012) Multigrain crystallography. Zeitschrift für Kristallographie, 227(1), 63-78.
Teter, D.M., Hemley, R.J., Kresse, G., and Hafner, J. (1998) High Pressure Polymorphism in Silica. Physical Review Letters, 80(10), 2145-2148.
Tse, J., Klug, D., and Le Page, Y. (1992) Novel high pressure phase of silica. Physical Review Letters, 69(25), 3647-3649.
Tsuchida, Y., and Yagi, T. (1990) New pressure-induced transformations of silica at room temperature. Nature, 347, 267-269.

Vaughan, G.B.M., Schmidt, S., and Poulsen, H.F. (2004) Multicrystal approach to crystal structure solution and refinement. Zeitschrift für Kristallographie, 219, 813-825.

Zhang, L., Meng, Y., Dera, P., Yang, W., Mao, W.L., and Mao, H.K. (2013) Single-crystal structure determination of (Mg,Fe)SiO3 postperovskite. Proc Natl Acad Sci U S A, 110(16), 6292-5.

Zhang, L., Meng, Y., Yang, W., Wang, L., Mao, W.L., Zeng, Q.S., Jeong, J.S., Wagner, A.J., Mkhoyan, K.A., Liu, W., Xu, R., and Mao, H.K. (2014) Disproportionation of (Mg,Fe)SiO(3) perovskite in Earth's deep lower mantle. Science, 344(6186), 877-82.

List of figure captions:

Figure 1. 100, 010 and 001 pole figures, representing the random orientations of six selected grains of seifertite for structure refinement. Compression axis in the DAC is along x_s and the sample was confined in a Re gasket along y_s and z_s.

Figure 2. XRD data of seifertite at 129 GPa and after *T* quench: (A) A representative spotty XRD pattern of seifertite coexisting with the dominant phase pPv at a fixed rotation angle (x-ray wavelength of 0.3738 Å), S-silica, pPv-post-perovskite, Ne-neon; (B) An integrated powder pattern at a fixed omega angle showing the intensity contrast between the major phase (Mg,Fe)SiO_3-pPv and seifertite (X-ray wavelength: 0.3738 Å). The characteristic peak 110 at 2.90 Å for seifertite is several times weaker than the major peaks from coexisting pPv.

Figure 3. Selected diffraction reflections from one grain of seifertite are shown in the middle within 30 by 30 pixels (pixel size: 79 μm) at 129 GPa: (A-B) the multigrain method distinguishes a pair of {302} reflections from another pair of {321} with close *d*-spacing; (C) a pair of weak {421} reflections with only a few pixels slightly more intense than the background can be picked out by the multigrain method.

411 **Table 1**. Calculated unit-cell parameters from multiple grains of seifertite at 129 GPa

412 and room *T*.

Parameters	**Grain1**	**Grain2**	**Grain3**	**Grain4**	**Grain1+2**	**Grain1+2+3**	**Grain1+2+3+4**
***a* (Å)**	3.72908	3.72933	3.72762	3.72537	3.72919	3.72862	3.72774
***σ*(*a*)**	0.00040	0.00030	0.00027	0.00027	0.00024	0.00018	0.00015
***B* (Å)**	4.65973	4.65857	4.65534	4.65754	4.65927	4.65765	4.65760
***σ*(*b*)**	0.00051	0.00060	0.00045	0.00054	0.00039	0.00027	0.00024
***c* (Å)**	4.16033	4.15955	4.16708	4.16019	4.15994	4.16076	4.16090
***σ*(*c*)**	0.00048	0.00049	0.00169	0.00083	0.00034	0.00033	0.00030
***V* (Å^3)**	72.2920	72.2653	72.3127	72.1839	72.2803	72.2583	72.2429
***σ*(*V*)**	0.0087	0.0095	0.0245	0.0106	0.0063	0.0055	0.0047
***N* (reflections)**	48	48	50	47	96	146	193

413

414

415

416

417

418

419

420

421

422 **Table 2**. Fractional coordinates of atoms and their isotropic thermal parameters.

423

Atom	*x*	*y*	*z*	Ueq
Si	0.0000	0.1504(3)	0.2500	0.0067(7)
O	0.7418(4)	0.6130(3)	0.919(1)	0.0069(8)

424

425 **Table 3**. Crystallographic data, parameters of structure refinements and interatomic
426 distances in comparison with previous studies.

Parameters	Multigrain This study	Theory Teter et al. (1998)	Theory Karki et al. (1997a, b)	Powder Dera et al. (2002)
P, GPa	129 GPa	120 GPa	120 GPa	0 GPa
a, Å	3.7277(2)	3.711	/	4.097(1)
b, Å	4.6576(2)	4.651	/	5.0462(9)
c, Å	4.1609(3)	4.159	/	4.4946(8)
*y*Si	0.1504(3)	0.1502	0.1501	0.1522(9)
*x*O	0.7418(4)	0.7424	0.7423	0.7336(19)
*y*O	0.6130(3)	0.6130	0.6134	0.6245(12)
*z*O	0.919(1)	0.9201	0.9201	0.9186(29)
Measured/independent/ free reflections	609/81/10	/	/	/
Refined parameters	15	/	/	/
R/R_{free}	0.056/0.064	/	/	/
R_{int}	0.096	/	/	0.034
Completeness	92.1%	/	/	/
Redundancy	6.6	/	/	/
Si-O	1.624(2) ×2	1.621×2	/	1.735×2
Si-O	1.655(3) ×2	1.650×2	/	1.783×2
Si-O	1.677(2) ×2	1.676×2	/	1.861×2

427

428

429 **Figure 1.**

430

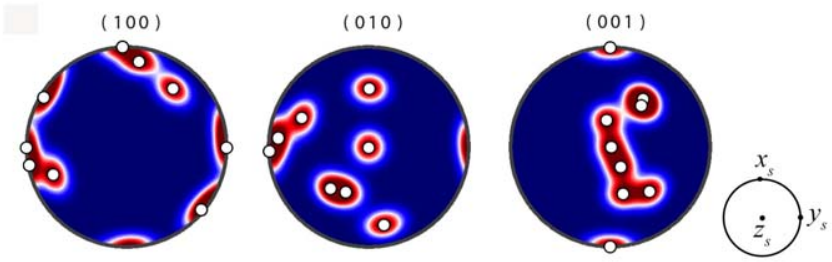

431

432

433

434 **Figure 2**.

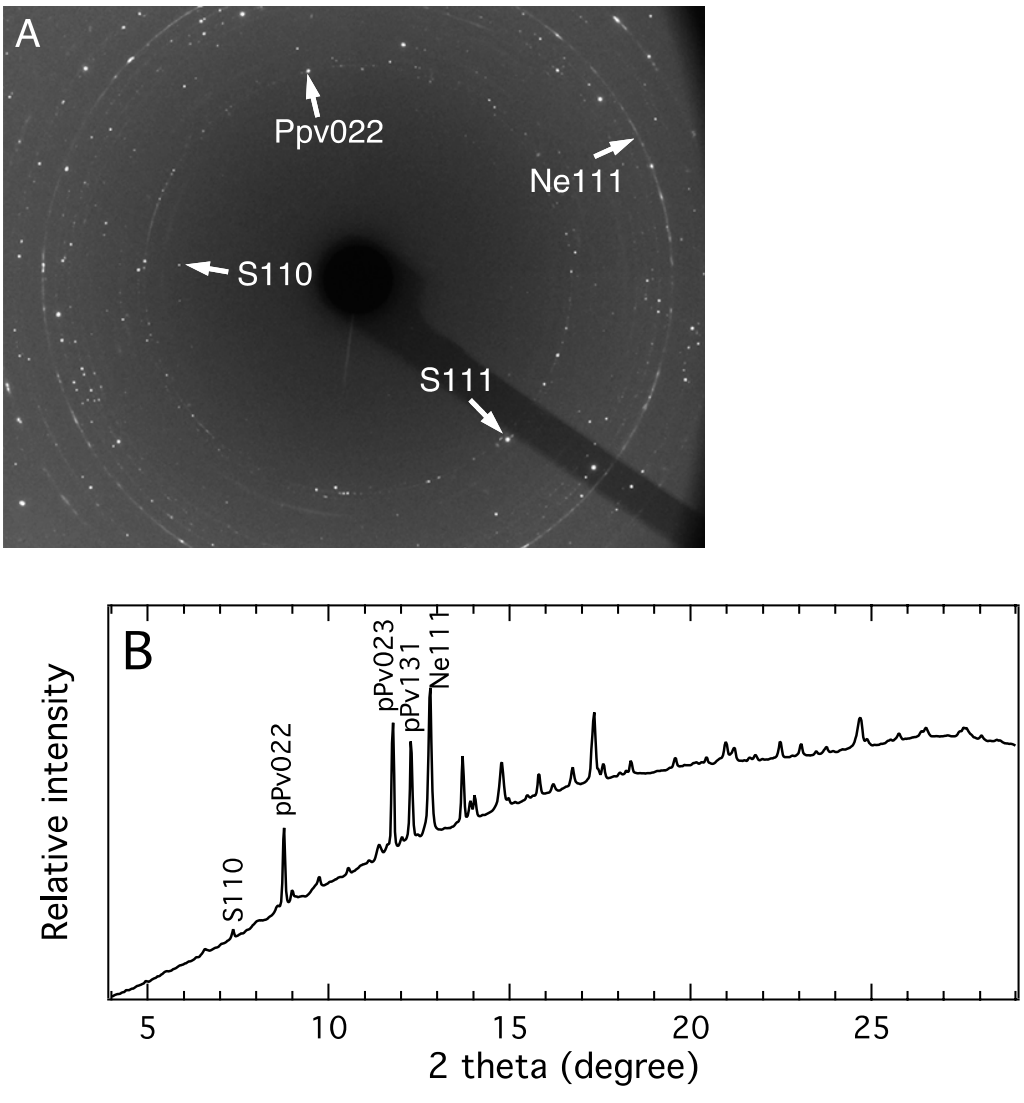

435

436

437

438

439

440 **Figure 3.**

441

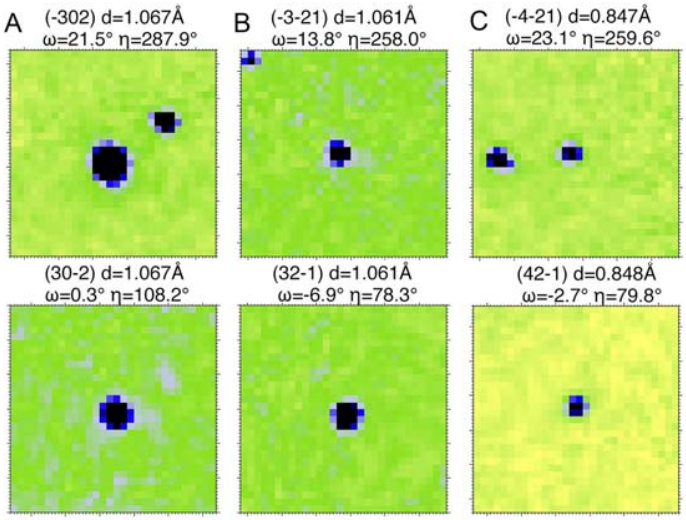

442

443